Highly efficient CRISPR systems for loss-of-function and gain-of-function research in pear calli

Meiling Ming¹, Hongjun Long¹, Zhicheng Ye¹, Changtian Pan², Jiali Chen¹, Rong Tian¹, Congrui Sun¹, Yongsong Xue¹, Yingxiao Zhang², Jiaming Li¹, Yiping Qi^{2, 3*}, Jun Wu^{1*}

*Correspondence: wujun@njau.edu.cn; yiping@umd.edu

¹College of Horticulture, State Key Laboratory of Crop Genetics and Germplasm Enhancement, Nanjing Agricultural University, Nanjing 210095, China.

²Department of Plant Science and Landscape Architecture, University of Maryland, College Park, Maryland 20742, USA.

³Institute for Bioscience and Biotechnology Research, University of Maryland, Rockville, Maryland 20850, USA.

© The Author(s) 2022. Published by Oxford University Press. All rights reserved. This is an Open Access article distributed under the terms of the Creative Commons Attribution License http://creativecommons.org/licenses/by/4.0/, which permits unrestricted reuse, distribution, and reproduction in any medium, provided the original work is properly cited.

E-mail addresses:

Meiling Ming (2017204012@njau.edu.cn); Hongjun Long (14819107@njau.edu.cn); Zhicheng Ye (2020804233@stu.njau.edu.cn); Changtian Pan (ctpan@umd.edu); Jiali Chen (14119221@njau.edu.cn); Rong Tian (14119207@njau.edu.cn); Congrui Sun (2019204012@njau.edu.cn); Yongsong Xue (2020204017@stu.njau.edu.cn); Yingxiao Zhang (zhyx89@gmail.com); Jiaming Li (lijiaming@njau.edu.cn); Yiping Qi (yiping@umd.edu, Phone: (301) 405-7682, Fax: (301) 314-9308); Jun Wu (Email: wujun@njau.edu.cn, Phone: 025-84396485, Fax: 025-84396485).

Running title: Targeted genome engineering in pear with CRISPR/Cas

Abstract

CRISPR/Cas systems have been widely used for genome engineering in many plant species, while their potentials have remained largely untapped in fruit crops, particularly in pear, due to the high levels of genomic heterozygosity and difficulties in tissue culture and stable transformation. To date, only few reports on application of CRISPR/Cas9 system in pear have been documented with a very low editing efficiency. Here, we report a highly efficient CRISPR toolbox for loss-of-function and gain-of-function research in pear. We compared four different CRISPR/Cas9 expression systems for loss-of-function analysis and identified a potent system that showed nearly 100% editing efficiency for multi-site mutagenesis. To expand targeting scope, we further tested different CRISPR/Cas12a and Cas12b systems in pear for the first time, albeit with low editing efficiency. In addition, we established a CRISPR activation (CRISPRa) system for multiplexed gene activation in pear callifor gain-of-function analysis. Furthermore, we successfully engineered the anthocyanin and lignin biosynthesis pathways using both CRISPR/Cas9 and CRISPRa systems in pear calli. Taken together, we build a highly efficient CRISPR

toolbox for genome editing and gene regulation, paving the way for functional genomics studies as well as molecular breeding in pear.

Keywords: CRISPR/Cas9, loss-of-function, CRISPRa, gain-of-function, pear, metabolic engineering

Introduction

CRISPR (clustered regularly interspaced short palindromic repeats)/Cas9 (CRISPR-associated protein), a Class 2 type II CRISPR system, can be easily programmed to introduce DNA double-strand breaking (DSB) at desired target site ¹. CRISPR/Cas9-mediated genome editing has been widely adopted across diverse species due to its high efficiency, specificity, simplicity, and versatility of multiplexing ²⁻⁵. In plants, CRISPR/Cas9-mediated genome editing has greatly advanced functional genomics and crop improvement ⁵⁻⁷. For example, CRISPR/Cas9 systems allow to shorten breeding cycles and accelerate plant domestication ^{8,9}, increase crop yield and improve food quality ^{10,11}, enhance resistance to biotic and abiotic stresses ^{12,13}, engineer metabolic pathways ^{14,15}, and break self-incompatibility ¹⁶

To achieve the full potential of CRISPR/Cas systems in plants, intense efforts have been made to improve editing efficiencies via optimizing expression cassettes and regulatory elements. Previous studies have demonstrated high activity of plant codon-optimized Cas9 driven by Pol II (RNA polymerase II) promoters, including Cauliflower mosaic virus (CaMV) 35S, ubiquitin, *YAO*, and the egg-cell specific promoter ¹⁷⁻¹⁹. The sgRNA (single guide RNA) expression is usually driven by a Pol III promoter such as U3 or U6 ¹⁷⁻¹⁹. However, these promoters have been demonstrated to be species-dependent for the efficiencies of CRISPR/Cas systems ^{20,21}

While the canonical CRISPR/Cas9 system recognizes an NGG protospacer adjacent motif (PAM) ²², Cas12 systems such as Cas12a (a Class 2 type V-A CRISPR system) and Cas12b (a Class 2 type V-B CRISPR system) prefer T-rich PAMs ^{23,24}. As the complements of Cas9, CRISPR/Cas12a and Cas12b systems have shown comparable activity and higher targeting specificity, allowing to generate staggered DSBs and larger deletions in many plant species ^{3,24}. Moreover, Cas12a is more suitable for multiplexed genome editing, since the CRISPR RNA (crRNA) array is short in length and can be processed by its RNase activity. LbCas12a and AaCas12b have been shown to be most reliable and efficient for genome editing in plants ²⁴⁻²⁷. Recently, a new Cas12a ortholog Mb2Cas12a has been reported in rice, showing relaxed PAM requirements, high editing activity and tolerant to relatively low temperatures ²⁸. However, neither CRISPR/Cas12a nor Cas12b systems have been demonstrated in pear.

Although CRISPR/Cas systems have been commonly used to generate loss-of-function mutations, they have also been repurposed as a programmable platform for gain-of-function analysis by transcriptional activation of target genes. The conventional gene overexpression approach by expressing the target gene with a constitutive promoter is laborious and challenging for multigene upregulation. CRISPRa systems, based on a deactivated Cas (dCas) protein fused with transcriptional activators, have shown efficient activation activity in several model plants ²⁹⁻³⁴. dCas protein has lost its ability to cut DNA due to mutations in the nuclease domain, but it remains competent for RNA-guided DNA binding without DSB in the target gene. The target gene is then activated by transcriptional activators without sequence mutation. Importantly, CRISPRa systems allow for simultaneous gene activation by assembling multiple sgRNAs targeting promoter regions of target genes. Recently, CRISPR-Act3.0, a third-generation CRISPRa system, showed potent single or multiplexed gene activation in rice, *Arabidopsis* and tomato ³⁵, further broadening the application of CRISPRa in plants.

Pear is an economically important fruit crop that belongs to the genus *Pyrus* in

the *Rosaceae* family and has been widely cultivated for > 3000 years in the world ³⁶. Genome editing holds a great promise to revolutionize pear genetics and breeding. Yet, only few studies have reported CRISPR/Cas9-mediated genome editing in pear and the editing efficiency remains very low ³⁷. In this study, we compared four different CRISPR/Cas9 expression systems and identified a potent system that showed nearly 100% editing efficiency even in a multiplexed setting using a stable transgenic pear callus system. Moreover, we benchmarked this efficient CRISPR/Cas9 system with comparison to different CRISPR/Cas12a and Cas12b systems in pear calli. As a demonstration, we successfully engineered anthocyanin and lignin biosynthesis by knocking out several key pathway genes in pear calli. To establish an effective gain-of-function system, we successfully applied CRISPR-Act3.0 system to activate genes involved in anthocyanin biosynthesis and observed phenotypic changes in pear calli. To our knowledge, this is the first demonstration of CRISPRa system in pear. In summary, this study successfully established efficient CRISPR systems for gene loss-of-function and gain-of-function studies in pear.

Results

Comprehensive analysis of four different CRISPR/Cas9 expression systems for genome editing in pear

To improve CRISPR/Cas9-mediated genome editing in pear, we constructed four different CRISPR/Cas9 expression systems (Fig. 1A), which allowed us to compare two Pol II promoters (35S and AtUBQ10) for Cas9 expression and two Pol III promoters (AtU3 and AtU6) for sgRNA expression. Four genes, *PyPDS*, *PyGID1*, *PyTFL1.1 and PyTFL1.2* were chosen as target genes. Loss-of-function of *PDS* (phytoene desaturase), *GID1* (gibberellic acid receptor) and *TFL1* (terminal flower 1) would produce albino ³⁷, dwarfing ³⁸ and early-flowering ³⁷ phenotypes, respectively. The *PyPDS*, *PyGID1* and *PyTFL1.1/1.2* DNA sequences of pear callus showed some SNPs (single nucleotide polymorphisms) compared to the reference genome

(Supplementary Fig. S1, S2 and S3). The DNA regions without SNPs were considered for targeted mutagenesis. We designed six and four sgRNAs targeting *PyPDS* and *PyGID1* exons, respectively (Supplementary Fig. S4A). Considering the high sequence identity between *PyTFL1.1* and *PyTFL1.2* (Supplementary Fig. S3), two sgRNAs (sgRNA01 and sgRNA02) were designed to target the common region of *PyTFL1.1* and *PyTFL1.2*, and one sgRNA (sgRNA03 or sgRNA04) was designed to specifically target *PyTFL1.1* or *PyTFL1.2* (Supplementary Fig. S4A). A total of 26 CRISPR/Cas9 T-DNA vectors were constructed to compare editing efficiencies using different Pol II and Pol III promoters in pear. In each T-DNA vector, two sgRNAs were simultaneously expressed to target each gene (Supplementary Fig. S4B).

We first tried *Agrobacterium*-mediated stable transformation of pear plants. A total of 2860 leaves were used for co-culture, and 1130 regenerated seedlings were harvested. However, no transgenic plant was identified by screening of 1130 regenerated seedlings with 3 mg/L hygromyein B (All seedlings died, data not shown), resulting from the extremely low transformation efficiency.

We next assessed these four different CRISPR/Cas9 expression systems for genome editing in stable dedifferentiated pear calli (Fig. 1B). The CRISPR/Cas9 components in the stable transgenic calli were detected using PCR with vector-specific primers (Supplementary Fig. S5). The resistance of T-DNA vectors pLR01-16 with Cas9 driven by AtUBQ10 promoter in plants is hygromycin, and pLR17-26 with Cas9 driven by 35S promoter is kanamycin. However, we found that 150 mg/L kanamycin had no selection pressure as compared to 15 mg/L hygromycin B for obtaining transgenic pear calli. We subsequently replaced the kanamycin resistance gene in T-DNA vectors pLR17-26 with the hygromycin resistance gene and renamed them to pLR55-64 (Supplementary Fig. S6B). During calli regeneration, a mass of regenerated calli highlighted by orange dotted circle is considered as an independent stable line (Fig. 1B). An independent stable line always contains more than one single cell. Stable transgenic callus lines were obtained for nearly all T-DNA vectors (Supplementary Fig. S5 and S6A). Mutation frequencies at *PyPDS*-gRNA05

site were first detected by PCR-restriction fragment length polymorphism (PCR-RFLP) and Sanger sequencing analysis (Supplementary Fig. S7). PCR-RFLP analysis showed that the vector pLR06 with AtU3 promoter exhibited 100% and 50% editing efficiencies in two randomly tested independent lines. By contrast, the vector pLR05 with AtU6 promoter exhibited no editing in two selected lines (Supplementary Fig. S7A). Sanger sequencing analysis further confirmed the results of PCR-RFLP analysis (Supplementary Fig. S7B).

To further assess the editing efficiencies of these four different CRISPR/Cas9 expression systems, we determined the mutation frequencies at all target sites in stable pear calli by high-throughput amplicon deep sequencing. Three to five independent lines were genotyped at each target site. In AtUBQ10-zCas9-mediated pear calli, mutation frequencies at five out of six sites of PvPDS were extremely high (nearly 100%) when sgRNAs were driven by AtU3 promoter (Fig. 1C). By contrast, mutation frequencies at the same sites of PyPDS were extremely low (nearly 0%) when sgRNAs were driven by AtU6 promoter (Fig. 1C). Consistently, mutation analysis of the other three target genes PyGID1 and PyTFL1.1/1.2 also showed that AtU3 promoter induced significantly higher editing efficiencies than AtU6 promoter (Fig. 1, D and E). These results suggest that AtU3 promoter outperforms AtU6 promoter for targeted mutagenesis in pear calli. Then we compared the efficiency of 35S and AtUBQ10 based Cas9 expression with AtU3-sgRNA module. At the five PyPDS sites and two PyGID1 sites, 35S and AtUBQ10 promoters induced comparable editing frequencies (Fig. 1, F and G). Impressively, mutation frequencies at eight out of fourteen test sites were nearly 100% when AtU3 was used for sgRNAs expression and AtUBQ10 was used for Cas9 expression (Fig. 1, C-E). Taken together, the combination of 35S- or AtUBQ10-Cas9 and AtU3-sgRNA modules represents a potent CRISPR/Cas9 system for loss-of-function analysis in pear.

Mutation types of the potent CRISPR/Cas9 systems

We assessed the mutation types of the two potent CRISPR/Cas9 systems, AtUBQ10-zCas9 and 35S-zCas9 coupled with AtU3-sgRNA. High-throughput sequencing results showed that both CRISPR/Cas9 systems mainly induce insertion and deletion mutations, which varied across the target sites (Fig. 2, A-C and Supplementary Fig. S8). For each target site, the occurrence and frequency of insertions and deletions were relatively consistent across five independent lines (Fig. 2, A-C), suggesting protospacer sequences largely dictate the editing outcomes. Occasionally, there is slight difference observed between AtUBQ10 and 35S promoters. For example, at *PyPDS*-gRNA02 site, Cas9 driven by AtUBQ10 mainly generated 1-2 base pair (bp) deletions, while Cas9 driven by 35S mainly generated 1 bp deletions (Fig. 2, D and E). Such difference might be attributed to discrepant activity of Cas9 in these two constructs. At this site, most frequent deletion position is the 4th base upstream of PAM site (Fig. 2, F and G) for both systems, one base pair upstream the DSB site.

CRISPR/Cas9 is far superior to Cas12a and Cas12b for genome editing in pear calli

To test CRISPR/Cas12a and Cas12b systems in pear, we focused on LbCas12a, Mb2Cas12a and AaCas12b, which showed high editing efficiencies in plants ^{24,25,28}. We expressed the rice codon optimized LbCas12a, Mb2Cas12a and AaCas12b with the AtUBO10 promoter. The crRNA (for Cas12a) or sgRNA (for Cas12b) array containing multiple crRNAs or sgRNAs flanked by hammerhead (HH) and hepatitis delta virus (HDV) ribozymes was expressed under a maize ubiquitin promoter (ZmUbi) (Fig. 3, A and F). We targeted exons of anthocyanin regulating genes, *PyMYB10* and *PyMYB114* ³⁹, and avoided all SNPs (Supplementary Fig. S9). For Cas12a, we designed six and five 23 nt crRNAs with TTTV PAMs for *PyMYB10* and *PyMYB114*, respectively. For Cas12b, we designed three 20 nt sgRNAs with VTTV PAMs for both *PyMYB10* and *PyMYB114* (Supplementary Fig. S10A). Two or four

crRNAs for Cas12a or two sgRNAs for Cas12b were simultaneously expressed in each T-DNA vector for single or multiplexed gene mutation (Supplementary Fig. S10B). The CRISPR/Cas12a and Cas12b components in the stable transgenic calli were first confirmed using PCR with vector-specific primers (Supplementary Fig. S11). In these transgenic calli, the editing efficiencies were relatively low for LbCas12a, Mb2Cas12a and AaCas12b (Fig. 3, B-E and G-H). To investigate whether higher temperature could improve the efficiency of LbCas12a, Mb2Cas12a and AaCas12b, the stable pear calli cultured at 25°C were then incubated at 30°C. After seven days of incubation, the editing efficiencies at all target sites remained at very low levels, although several of them were enhanced (Fig. 3, B-E and G-H). These data demonstrated that, comparing with CRISPR/Cas9, the current CRISPR/Cas12a and Cas12b systems need to be optimized for genome editing in pear. With such comparison, we have benchmarked our highly efficient CRISPR/Cas9 system as the preferred genome editing system in pear.

Highly efficient multiplexed editing of anthocyanin and lignin biosynthetic genes in pear calli

A callus system can accelerate the process of gene functional study, because it is a homologous system amenable by genetic engineering ⁴⁰⁻⁴³. We reasoned that application of our highly efficient CRISPR/Cas9 system in stable pear calli represents an effective genetic method for gene functional studies in pear. To demonstrate such an application, we constructed five CRISPR/Cas9 vectors targeting *PyMYB10*, *PyMYB114*, *PyMYB169* and *PyNSC* (Fig. 4A). *PyMYB10* and *PyMYB114* are key transcription factors that involved in enhancing anthocyanin biosynthesis, while *PyMYB169* and *PyNSC* are important transcription factors that involved in enhancing lignin biosynthesis ^{39,44,45}. Analysis of *PyMYB10*, *PyMYB114*, *PyMYB169* and *PyNSC* DNA sequences in pear calli showed that there are some SNPs compared to the reference genome (Supplementary Fig. S9 and S12). We designed three or two

sgRNAs targeting exons without SNPs (except for PvNSC-gRNA03) for each target gene (Supplementary Fig. S13A). Noted that there is 1 bp mismatch nucleotide in PyNSC-gRNA03, which was intentionally designed to assess targeting specificity (Supplementary Fig. S12B and S13A). Two sgRNAs were simultaneously expressed in each T-DNA vector for single or multiplexed gene mutation (Supplementary Fig. S13B). The T-DNA vectors pLR89, pLR90 and pLR91 were designed to target PyMYB10 and PyMYB114 simultaneously. The T-DNA vectors pLR92 and pLR94 were designed to target PyMYB169 and PyNSC, respectively (Supplementary Fig. S13B). The CRISPR/Cas9 components in the stable pear calli were detected using PCR with vector-specific primers (Supplementary Fig. S14). Two to three independent transgenic lines were genotyped at each target site by Sanger sequencing. Overall, mutation frequencies at all target sites were very high (80% to 100%) except the PyMYB10-gRNA02 site with 50% editing efficiency (Fig. 4B). For PyNSC-gRNA03 with 1 bp mismatch nucleotide, none of the three transgenic callus lines showed detectable editing (Fig. 4B and Supplementary Fig. S16), suggesting high specificity of the CRISPR/Cas9 system. Impressively, mutation frequencies at six out of nine sites were up to 100% (Fig. 4B). Further mutation analysis revealed that 1 bp insertions and deletions have occurred predominantly at most of target sites (Fig. 4C and Supplementary Fig. S15, S16). Some large deletions (more than 20 bp) were also identified at some target sites by Sanger sequencing (Supplementary Fig. S15 and S16).

Such high-frequency targeted mutagenesis suggests that we can easily generate loss-of-function callus mutants for genetic studies. To this end, we selected the knockout callus lines of *PyMYB10* and *PyMYB114* for phenotypic characterization. The wild-type (WT) calli and calli harboring T-DNA vector without sgRNA (EV) were used as controls (CTRL). The pear calli were grown on treatment medium under a continuous light condition at 17°C. The treatment medium was Murashige and Skoog (MS) solid medium without nitrogen but containing 200 µM/L of Methyl jasmonate (MeJA). After seven days of treatment, the CTRL pear calli appeared red,

indicating strong accumulation of anthocyanin, whereas the calli with CRISPR/Cas9-mediated *PyMYB10* and *PyMYB114* knocked out showed no or weak accumulation of anthocyanin (Fig. 4, D and E). Consequently, the expression levels of anthocyanin biosynthesis-related enzyme-encoding genes *PyDFR*, *PyANS* and *PyUFGT* were substantially lower in the *PyMYB10* and *PyMYB114* knockout calli than in CTRL (Fig. 4F), suggesting these genes are regulated by *PyMYB10* and *PyMYB114* ³⁹.

We also identified the phenotypes of CRISPR/Cas9-mediated *PyMYB169* or *PyNSC* knockout calli. The WT calli and EV calli were used as controls (CTRL). The pear calli were grown under continuous dark conditions at 25°C for 20 days. After 20 days of incubation, the calli were stained by phloroglucinol-HCl (Wiesner reagent) to indicate the lignin contents by a red-purple color ⁴⁶. Compared to CTRL pear calli with red-purple color, no red-purple color of lignin staining was observed in CRISPR/Cas9-mediated *PyMYB169* or *PyNSC* knockout calli (Fig. 4, G and H). As expected, the expression levels of the major lignin pathway genes, including *Py4CL1*, *PyC3H1*, *PyCSE*, *PyHCT2*, *PyCCOMT2*, *PyCAD*, *PyF5H*, *PyPOD2* and *PyLAC1*, were reduced in *PyMYB169* or *PyNSC* knockout calli (Fig. 4I). Taken together, by engineering the anthocyanin and lignin biosynthesis, we demonstrate that our CRISPR/Cas9 system represents an efficient tool for loss-of-function studies, contributing to bridging phenotype-genotype gap in pear.

Efficient singular and multiplexed gene activation by CRISPR-Act3.0 for gain-of-function studies in pear calli

A third-generation CRISPRa system, CRISPR-Act3.0 ³⁵ was adapted in this study for gene activation. Based on our findings in CRISPR/Cas9 assays, the Pol II promoter AtUBQ10 and Pol III promoter AtU3 were employed to express dCas9 and sgRNAs, respectively, for the CRISPRa system in pear (Fig. 5A). For the structure of CRISPR-Act3.0, the dCas9 was fused with an activation domain VP64, and the

coupled sgRNA2.0 scaffold contained two MS2 aptamers for recruiting the MS2 bacteriophage coat protein (MCP), which was fused to the 10xGCN4 SunTag⁴⁷. As the GCN4's antibody, the single-chain variable fragment (scFv) fused with a super folder green fluorescent protein (sfGFP) and 2xTAD activator can be recruited to the SunTag (Fig. 5B). Two or four different sgRNAs were designed to target the promoters of PybZIPa, PyMYB10, PyMYB114, PybHLH3, PyDFR, PyANS or PyUFGT, all these genes were identified related to anthocyanin biosynthesis. PybZIPa, PyMYB10, PyMYB114 and PybHLH3 are important transcription factors that involved in regulating anthocyanin biosynthesis, while PyDFR, PyANS and PyUFGT are enzyme-encoding genes of anthocyanin pathway^{39,48} (Supplementary Fig. S17A). Two to six sgRNAs were simultaneously expressed in each T-DNA vector for single or multiplexed gene activation (Supplementary Fig. \$17B). The CRISPR/dCas9 components in the stable transgenic calli were detected using PCR with vector-specific primers (Supplementary Fig. \$18). Quantitative RT-PCR analysis showed that four out of seven genes were activated 10-fold or higher in some lines with specific sgRNAs (Fig. 5, C-F). PvbZIPa were activated up to 40-fold in some lines (Fig. 5C). PyMYB114 and PybHLH3 were simultaneously activated by 10-fold to 20-fold in calli with the T-DNA vector pLR50 (Fig. 5D and Supplementary Fig. S17B). While *PyMYB10* and *PybHLH3* were only slightly activated in calli (around 2to 6-fold) with both the T-DNA vector pLR51 and pLR52 (Fig. 5E and Supplementary Fig. S17B). For simultaneous *PyDFR*, *PyANS* and *PyUFGT* activation, *PyUFGT* were activated by 10- to 40-fold in most lines, whereas PvDFR and PvANS were only activated 2- to 10-fold in the same lines (Fig. 5F). These results demonstrate that the CRISPR-Act3.0 mediated activation is sgRNA- or gene-specific in pear.

The stable callus lines with high levels of gene activation (highlighted by black dotted box) were cultured on treatment medium under continuous light conditions at 17°C for phenotype identification (Fig. 5, C, D and F). The treatment medium was MS solid medium containing 50 μ M/L of MeJA. The WT calli and calli harboring T-DNA vectors without sgRNA (EV) were used as control (CTRL). After

12 days of incubation, CTRL calli showed no or very weak red color and a low anthocyanin content (Fig. 5, G and H). However, most of calli with CRISPR-Act3.0-mediated PybZIPa, PyMYB114 and PybHLH3 or PyDFR, PyANS and PvUFGT activation appeared red and had a strong or moderate accumulation of anthocyanin (Fig. 5, G and H), which are anticipated phenotypes for gain-of-function of these genes. Moreover, the expression levels of anthocyanin pathway enzyme-encoding genes PyDFR, PyANS and PyUFGT were up-regulated in CRISPR-Act3.0-mediated calli compared to CTRL (Fig. 5I).

Targeting specificity of CRISPR/Cas9 systems in pear calli

To assess the specificity of our CRISPR/Cas9 systems in pear, we selected five target sgRNAs for off-target analysis in stable calli (Table 1). Ten top potential off-target sites were identified by Cas-OFFinder ⁴⁹. Each potential off-target site contained 2-3 mismatches and was genotyped in one transgenic callus line by Sanger sequencing. Off-target mutations were detected at two out of ten potential off-target sites. Both off-target sequences contain less than 2 mismatches at the PAM proximal 12-nt "seed" sequence, showing 40% and 60% off-target mutation frequencies, respectively (Table 1 and Supplementary Fig. S19). All other potential off-target sequences with 2 or 3 mismatches within the seed sequence of protospacer had no mutations in pear calli (Table 1 and Supplementary Fig. S19). Therefore, to ensure high targeting specificity, it is preferrable to design sgRNAs whose closest off-target sites contain more than 2 bp mismatch nucleotides within the protospacer seed sequence.

Discussion

Highly efficient genome editing can be obtained in stable pear calli by CRISPR/Cas9 systems with AtU3 promoter but not AtU6 promoter

In the past decade, many efforts have been made to improve CRISPR/Cas9 editing

efficiency in plants, particularly those have complex genome and lack of an efficient stable transformation system. Editing efficiency of CRISPR/Cas9 systems could be improved through enhancing the expression level of Cas9 and sgRNAs ²¹. The application of improved Pol II promoters (35S, ubiquitin, *YAO*, or the egg-cell specific promoter) and Pol III promoters (U3 or U6) is an effective strategy for enhancing the expression of Cas9 and sgRNAs in plants ^{18,19,21}. For example, the CRISPR/Cas9 system with PcUbi4-2 expressing Cas9 and MdU3/U6 expressing sgRNAs led to higher editing efficiency (84-93%) in apple ³⁷. The CRISPR/Cas9 system with 35S promoter expressing Cas9 and AtU6-1 expressing sgRNAs only generated moderate editing efficiency (31.8%) in apple ⁵⁰. For sgRNAs expression, both AtU6-26 promoter and FveU6-2 promoter showed high-efficiency genome editing in strawberry ⁵¹. The sgRNAs driven by VvU3/U6 promoters resulted in higher editing efficiency in grape cells (14.65-22.10%) than sgRNAs driven by AtU6 promoter (13.67%) ²¹.

Application of CRISPR/Cas systems in pear was challenging because of the highly heterozygous genome and inefficient stable transformation method ^{36,37}. In this study, we used the maize codon optimized Cas9, which is highly efficient for genome editing in *Arabidopsis* ⁵², rice ⁵³, maize ⁵⁴, wheat ⁵⁵, tomato ⁵⁶, and poplar ²⁰. We compared four different CRISPR/Cas9 systems containing two Pol II promoters (35S and AtUBQ10) for Cas9 expression and two Pol III promoters (AtU3 and AtU6) for sgRNAs expression in stable pear calli (Fig. 1A). We found that both 35S and AtUBQ10 promoters induced extremely high editing efficiencies (nearly 100%) when sgRNAs were driven by AtU3 promoter (Fig. 1, F and G). By contrast, poor editing efficiencies were observed with AtU6 promoter expressing sgRNAs, regardless the promoter is more efficient than AtU6 promoter for CRISPR/Cas9 systems in pear. It is consistent with the recent observations that AtU3 outperforms AtU6 for Cas9 mediated genome editing in tomato ⁵⁶ and poplar ²⁰. Our established CRISPR/Cas9 system resulted in high editing efficiencies (nearly 100%) in pear calli.

Because of the bottlenecks in tissue culture and stable transformation, only proof-of-concept for CRISPR/Cas9 gene-editing had been conducted in fruit crops mainly based on the gene *PDS* rather than trait-related genes, such as in citrus ⁵⁷, apple ⁵⁰, grape ⁵⁸, kiwifruit ⁵⁹, banana ^{60,61}, strawberry ^{62,63} and pear ³⁷. Recently, increasing CRISPR studies focused on improving the editing efficiency, enhancing the resistance to biotic and abiotic stresses, promoting early flowering and dwarfing, and gene functional studies have been reported in fruit crops ^{9,21,64,65}. However, to our knowledge, our CRISPR/Cas9 system developed in pear represent the highest efficient CRISPR system in fruit tree crops: 93% in apple ³⁷, 43.24% in grape ²¹, 64.7% in citrus ⁶⁶, 75% in kiwifruit ⁹. Hence, we have a highly efficient CRISPR/Cas9 system that may be applicable to other fruit tree crops.

CRISPR/Cas12a and Cas12b are low efficient for genome editing in pear

The canonical CRISPR/Cas9 recognizes an NGG PAM ²², while CRISPR/Cas12a and Cas12b prefer T-rich PAMs ^{23,24}, contributing to expand targeting scope. Importantly, CRISPR/Cas12a and Cas12b systems have shown comparable activity and higher targeting specificity than CRISPR/Cas9 in many plant species, such as in rice ^{24,25,28,67}, maize ⁵⁴, cotton ^{68,69} and citrus ⁷⁰. It's worth noting that the aforementioned species are general thermophilic crops, which need relatively high temperatures (above 30°C) for tissue culture and growth. Previous studies demonstrated that both Cas12a and Cas12b nucleases are temperature sensitive and they require a temperature of more than 28 °C for high activity 71,72. Therefore, CRISPR/Cas12a and Cas12b systems induced relatively low editing efficiency in dicotyledon which typically grow at or lower than 25°C. For example, CRISPR/LbCas12a had no editing activity at 22°C in Arabidopsis, but the editing efficiency increased to 35% under 29°C treatment for one month 71. In this study, we found that both CRISPR/Cas12a and Cas12b systems including LbCas12a, Mb2Cas12a and AaCas12b were low efficient for editing in pear calli cultured at 25°C (Fig. 3, B-E and G-H). Their editing efficiencies were not induced or only slightly enhanced after the stable pear calli were incubated at 30°C for 7 days (Fig. 3,

B-E and G-H). These results indicate that a long-term high-temperature treatment might be critical to improving editing efficiencies of CRISPR/Cas12a and Cas12b systems in pear. However, the pear calli could not survive under long-period high-temperature conditions, preventing us from further optimizing CRISPR/Cas12a and Cas12b systems in pear. In the future, temperature-insensitive Cas12a and Cas12b variants are needed to be developed for genome editing in pear.

Potent CRISPR/Cas9 system is a powerful tool for gene loss-of-function studies in pear

Targeted mutagenesis by genome editing tools such as CRISPR/Cas9 is an efficient approach to probe the causal relationships between genotype and phenotype in plants. However, the application of CRISPR/Cas systems in fruit crops is still in its infancy due to the high levels of genomic heterozygosity and challenges in tissue culture and stable transformation^{7,73}. Callus is a good system for such reverse genetics analysis in fruit trees as it bypasses the lengthy plant regeneration and juvenile stage. In addition, the efficiency of stable transformation of callus is usually very high, and transgenic calli can be obtained through a short screening time, which could accelerate the gene function studies in fruit crops. In this study, we showed highly efficient multiplexed editing (nearly 100%) of anthocyanin and lignin biosynthetic genes by assembling multiple sgRNA expression cassettes into single T-DNA vectors (Fig. 4B). The phenotypes of pear calli were consistent with genotyping results (Fig. 4, D and G), suggesting that the established CRISPR/Cas9 system allows for rapid loss-of-function analysis in pear. Recently, CRISPR/Cas9 systems-mediated high-throughput functional genomics screening has been implemented in several crops including rice 74.75, tomato 76, maize 77, and soybean 78. The high editing efficiency of our CRISPR/Cas9 system would enable us to perform high-throughput functional genomics study in pear. Undoubtedly, our CRISPR/Cas9 system will advance the understanding of various developmental processes such as anthocyanin, lignin, sugar, acid, aroma accumulation as well as biotic and abiotic stress responses, which could be fully studied using pear calli. This study also provides a valuable model for other species without a stable plant transformation system. At the same time, genome editing using callus system has its own limitations. For example, some specific phenotype research such as dwarfing and flowering are unachievable using callus system. But, it is conceivable that an embryogenic callus may be used if regeneration of the whole plant is needed for phenotypic analysis.

CRISPRa system is a powerful tool for gain-of-function study in pear

Calli have been widely used in gene functional studies in fruit crops mainly via the conventional gene overexpression approach 41-43,79,80, due to its high efficiency and fast detection in transgenic lines. CRISPRa systems outperformed the conventional gene overexpression approach, due to the convenience of expressing multiple sgRNAs 32,35. In this study, we achieved efficient singular and multiplexed gene activation with CRISPR-Act3.0 using AtUBQ10 and AtU3 promoters. Consistent with the previous observation in rice ³⁵, different sgRNAs targeting the same gene could resulted in large variation of activation efficiency, suggesting the significance of sgRNA design (Fig. 5, C-F and Supplementary Fig. S17). Furthermore, some genes are easier than others for CRISPRa-induced transcriptional activation, which might be resulted from the discrepant transcriptional control mechanisms imposed on different genes. Nevertheless, our results suggest CRISPRa system is a powerful tool for gene activation that can render phenotypic changes as gain-of-function in pear (Fig. 5G). However, it is recommended to assess multiple sgRNAs for each target genes to identify the most potent sgRNAs. With our stable callus system, it is possible to fast screen the sgRNA activity for activation, which will ultimately help achieve high level gene activation in pear.

In conclusion, we have established a highly efficient CRISPR/Cas9 system for genome editing in pear, which is preferred over CRISPR/Cas12a and Cas12b systems. We successfully applied it for gene loss-of-function studies using a pear callus system. Furthermore, we demonstrated efficient singular and multiplexed genes activation by

CRISPR-Act3.0. Overall, this study provided a CRISPR toolbox that will aid loss-of-function and gain-of-function research in pear and potentially other fruit crops.

Materials and methods

Plant materials and growth conditions

Dedifferentiated pear calli were induced from *Pyrus communis* based on the previous report ⁴². The calli were cultured on Murashige and Skoog (MS) solid medium containing 1.0 mg/L of 2, 4-dichlorophenoxy (2, 4-D) and 0.5 mg/L of N6-benzyladenine (6-BA) under continuous dark conditions at 25°C and subcultured every 2 weeks. Pear plants were grown on MS solid medium containing 1.0 mg/L of 6-BA and 0.2 mg/L of Indole-3-butytric acid (IBA) at 25°C with a 16h-light/8h-dark photoperiod and subcultured every month.

Vector construction

All T-DNA expression vectors were constructed based on a Golden Gate cloning and three-way Gateway cloning system as previously described ^{24,28,35}. Briefly, each sgRNA of target gene was first cloned into sgRNA expression cassette pYPQ131 or pYPQ132 or pYPQ133 or pYPQ134 by T4 DNA ligase. Then, multiple sgRNA cassettes were assembled into sgRNA expression vector pYPQ142 or pYPQ143 or pYPQ144 by Golden Gate reactions to simultaneously express multiple sgRNAs in one T-DNA vector. Finally, the sgRNA expression vector containing multiple sgRNAs and CRISPR-Cas9/dCas9/Cas12a/Cas12b expression cassette were cloned into destination backbone vector pYPQ202 (hygromycin resistance) or pCGS710 (kanamycin resistance) to generate the final T-DNA expression vectors (such as pLR01, pLR02 and so on) by Three-way LR reaction. All backbone vectors used in this study are available from Addgene: pYPQ131A (no.69273), pYPQ132A (no.69274), pYPQ131B (no.69281), pYPQ132B (no.69282), pYPQ131-STU-Fn

(no.138095), pYPQ132-STU-Fn (no.138098), pYPQ133-STU-Fn (no.138101), pYPQ134-STU-Fn (no.138104), pYPQ131-STU-Lb (no.138096), pYPQ132-STU-Lb (no.138099), pYPQ133-STU-Lb (no.138102), pYPQ134-STU-Lb (no.138105), pYPQ131B2.0 (no.99885), pYPQ132B2.0 (no.99888), pYPQ133B2.0 (no.99892), pYPQ142 (no.69294), pYPQ143 (no.69295), pYPQ144 (no.69296), pYPQ141-ZmUbi-RZ-Aac (no.129685), pYPQ144-ZmUbi-pT (no.138108), pYPQ166 (no.109328), pYPQ230 (no.86210), pYPQ284 (no.138116), pYPQ292 (no.129672), pYPQ-dzCas9-Act3.0 (no.158414), pYPQ202 (no.86198).

Stable transformation of pear calli and pear plants

For the stable transformation assays, the final T-DNA expression vectors (such as pLR01, pLR02 and so on) were transformed into Agrobacterium tumefaciens strain GV3101 using the freeze-thaw method, according to the manufacturer's instructions (Weidi, http://www.weidibio.com). For stable transformation of pear calli, Agrobacterium cells were resuspended in the MS liquid medium with 100 mM AS to an OD₆₀₀ of 0.6 to 0.8, and then incubated at room temperature with slow shaking for 1 h. Dedifferentiated pear calli were then incubated in the Agrobacterium suspension for 15 min. The T-DNA vector without sgRNA (EV) was transformed as negative control. After infiltration, calli were incubated on MS solid medium with 100 mM AS under dark conditions at 25°C for two days. Then calli were transferred to MS solid medium with 15 mg/L hygromycin B and 150 mg/L cefotaxime for transgenic calli selection. After a month, the regenerated calli were collected and subcultured every 15 days for genotyping and phenotyping. During calli regeneration, a mass of regenerated calli highlighted by orange dotted circle is considered as an independent stable line (Fig. 1B), an independent stable line always contains more than one single cell.

For stable transformation of pear plants, leaves were wounded with a scalpel and preincubated on NN69 (NITSCH and NITSCH 1969) solid medium containing

3.0 mg/L of thidiazuron (TDZ) and 0.3 mg/L of IBA under dark conditions at 25°C for 5 days. *Agrobacterium* cells were resuspended in the NN69 liquid medium with 100 mM AS to an OD₆₀₀ of 0.6. The pre-wounded leaves were dipped into the inoculum with slow shaking for 20 mins, followed by co-culturing on NN69 solid medium containing 3.0 mg/L of TDZ, 0.3 mg/L of IBA and 100 mM AS under dark conditions at 25°C for two days. At the end of co-cultivation, leaves were plated on NN69 solid medium containing 3.0 mg/L of TDZ, 0.3 mg/L of IBA and 150 mg/L cefotaxime at 25°C under continuous dark conditions. Noted that the leaves were always plated abaxial side down on solid medium. One month later, the regenerated plants were transferred to grown medium containing 150 mg/L cefotaxime and 3 mg/L hygromycin B and subcultured every month for genotyping and phenotyping.

Mutation analysis by PCR-RFLP, Sanger sequencing and high-throughput sequencing

Pear calli were collected for genomic DNA extraction using the CTAB (cetyl trimethylammonium bromide) method. The genomic regions flanking the target sites were PCR amplified for PCR-RFLP analysis, Sanger sequencing and high-throughput sequencing. First, the CRISPR/Cas components in the stable transgenic calli were detected using PCR with vector-specific primers. Then, Cas nucleases-induced mutations were detected by PCR-RFLP and followed by Sanger sequencing or high-throughput sequencing. For PCR-RFLP analysis, PCR amplicons were digested with corresponding restriction enzymes and visualized on 1.5% TAE agarose gels. ImageJ (https://imagej.nih.gov/ij/) was used to quantify the mutation frequencies. PCR amplicons were cloned into the pMD19-T vector for Sanger sequencing. Editing frequencies were calculated by the number of mutated clones divide by the number of total sequenced clones. For high-throughput amplicon deep sequencing, PCR amplicons with sequencing barcodes were sent to Novogene for quality check and followed by high-throughput sequencing using an Illumina HiseqX-PE150 platform.

Clean sequencing data were analyzed by CRISPRMatch ⁸¹ for mutation frequencies and profiles. The total mutation ratio at each target site was calculated by dividing the mutant reads (include deletion and insertion) by the total reads. For off-target analysis, Cas-OFFinder ⁴⁹ was used to identify potential off-target sites. To detect possible mutations, PCR amplicons were also cloned into the pMD19-T vector for Sanger sequencing.

RNA extraction and qRT-PCR analysis

Total RNA was extracted from transgenic calli with the Plant Total RNA Isolation manufacturer's instructions Plus Kit, according the (Foregene, http://www.foregene.com). First-strand cDNA was synthesized with EasyScript® First-Strand cDNA Synthesis SuperMix Kit and qRT-PCR assay was conducted with TransStart[®] SuperMix Green qPCR. (Transgene, https://www.transgen.com.cn/rt pcr.html) using a real-time LightCycler 480 II® PCR detection system (Roche). The transcript expression levels were determined by the $2^{-\Delta\Delta Ct}$ method. PyGAPDH was used as the endogenous control genes. All primers used in this study are listed in Supplementary Table S1.

Phenotyping, extraction and measurement of anthocyanin and lignin

Based on the different purposes, the different cultural conditions were employed in phenotyping analysis. For CRISPR/Cas9-mediated *PyMYB10* and *PyMYB114* knockout calli, the stable pear calli were cultured on MS solid medium without nitrogen but containing 200 μM/L of MeJA under continuous light conditions at 17°C for 7 days before anthocyanin analysis. For CRISPRa-mediated activation of anthocyanin biosynthetic genes in calli, the stable pear calli were cultured on MS solid medium containing 50 μM/L of MeJA under continuous light conditions at 17°C for 12 d before anthocyanin analysis. The total anthocyanin was extracted and

measured as described in our previous report ³⁹.

For CRISPR/Cas9-mediated *PyMYB169* or *PyNSC* knockout calli, the stable pear calli were cultured on MS solid medium containing 100 µM/L brassinolide (BR) but no 2, 4-D and 6-BA under continuous dark conditions at 25°C for 20 days before lignin analysis ⁸². The total lignin was extracted and measured as described in our previous report ⁴⁴. Noted that there is no lignin biosynthesis in pear calli if 2, 4-D and 6-BA are added to the MS solid medium.

Data availability. The high-throughput sequencing data sets have been submitted to the National Center for Biotechnology information (NCBI) database under Sequence Read Archive (SRA) BioProject ID: PRJNA787753.

Author contributions

J. W and M.M designed the experiments. J. W and Y. Q supervised the research. M. M, C. P and Y. Z generated all the vectors. M. M, H. L, Z. Y, J. C, R. T and J. L performed the stable transformation of pear calli and plants. M. M did all genotyping and phenotyping analysis with the help of C. S and Y. X. J. W, Y. Q and M. M wrote the paper with input from other authors. All authors read and approved the final manuscript.

Acknowledgements

This work was supported by grants from the National Science Foundation of China (31820103012, 31725024), the National Key Research and Development Program (2018YFD1000200), the Earmarked fund for China Agriculture Research System (CARS-28), the Earmarked Fund for Jiangsu Agricultural Industry Technology System JATS [2021]453. This work was also supported by the National Science

Foundation Plant Genome Research Program grant (IOS-1758745) to Y. Q. H. L, J. C, R. T were supported by a scholarship from National Training Program of Innovation and Entrepreneurship for Undergraduates (202110307017). We thank the Centre of Pear Engineering Technology Research, State Key Laboratory of Crop Genetics and Germplasm Enhancement, Nanjing Agricultural University for supporting this project.

Conflict of interests

The authors declare that they have no conflicts of interest.

References

- Hsu, P. D., Lander, E. S. & Zhang, F. Development and applications of CRISPR-Cas9 for genome engineering. *Cell* **157**, 1262-1278 (2014).
- Hille, F. et al. The Biology of CRISPR-Cas: Backward and Forward. Cell 172, 1239-1259 (2018).
- Zhang, Y., Malzahn, A. A., Sretenovic, S. & Qi, Y. The emerging and uncultivated potential of CRISPR technology in plant science. *Nat Plants* 5, 778-794 (2019).
- Zhou, J. *et al.* Application and future perspective of CRISPR/Cas9 genome editing in fruit crops. *J Integr Plant Biol* **62**, 269-286 (2020).
- 5 Zhu, H., Li, C. & Gao, C. Applications of CRISPR-Cas in agriculture and plant biotechnology. *Nat Rev Mol Cell Biol* **21**, 661-677 (2020).
- 6 Chen, K., Wang, Y., Zhang, R., Zhang, H. & Gao, C. CRISPR/Cas Genome Editing and Precision Plant Breeding in Agriculture. *Annu Rev Plant Biol* **70**, 667-697 (2019).
- Wang, T., Zhang, H. & Zhu, H. CRISPR technology is revolutionizing the improvement of tomato and other fruit crops. *Hortic Res* **6**, 77 (2019).
- 8 Li, T. *et al.* Domestication of wild tomato is accelerated by genome editing. *Nat Biotechnol* **36**, 1160-1163 (2018).
- 9 Varkonyi-Gasic, E. *et al.* Mutagenesis of kiwifruit CENTRORADIALIS-like genes transforms a climbing woody perennial with long juvenility and axillary flowering into a compact plant with rapid terminal flowering. *Plant Biotechnol J* **17**, 869-880 (2019).
- Xing, S. et al. Fine-tuning sugar content in strawberry. Genome Biol 21, 230 (2020).
- Zhang, J. *et al.* Increasing yield potential through manipulating of an ARE1 ortholog related to nitrogen use efficiency in wheat by CRISPR/Cas9. *J Integr Plant Biol* **63**, 1649-1663 (2021).
- Wang, L. *et al.* CRISPR/Cas9-mediated editing of CsWRKY22 reduces susceptibility to Xanthomonas citri subsp. citri in Wanjincheng orange (Citrus sinensis (L.) Osbeck). *Plant Biotechnology Reports* **13**, 501-510 (2019).
- Tao, H. *et al.* Engineering broad-spectrum disease-resistant rice by editing multiple susceptibility genes. *J Integr Plant Biol* **63**, 1639-1648 (2021).
- Deng, L. et al. Efficient generation of pink-fruited tomatoes using CRISPR/Cas9 system. J

- Genet Genomics 45, 51-54 (2018).
- Yan, S. *et al.* Anthocyanin Fruit encodes an R2R3-MYB transcription factor, SIAN2-like, activating the transcription of SIMYBATV to fine-tune anthocyanin content in tomato fruit. *New Phytol* **225**, 2048-2063 (2020).
- Ye, M. *et al.* Generation of self-compatible diploid potato by knockout of S-RNase. *Nat Plants* **4**, 651-654 (2018).
- Ma, X. *et al.* A Robust CRISPR/Cas9 System for Convenient, High-Efficiency Multiplex Genome Editing in Monocot and Dicot Plants. *Mol Plant* **8**, 1274-1284 (2015).
- Wang, Z. P. *et al.* Egg cell-specific promoter-controlled CRISPR/Cas9 efficiently generates homozygous mutants for multiple target genes in Arabidopsis in a single generation. *Genome Biol* **16**, 144 (2015).
- Yan, L. *et al.* High-Efficiency Genome Editing in Arabidopsis Using YAO Promoter-Driven CRISPR/Cas9 System. *Mol Plant* **8**, 1820-1823 (2015).
- Li, G., Sretenovic, S., Eisenstein, E., Coleman, G. & Qi, Y. Highly efficient C-to-T and A-to-G base editing in a Populus hybrid. *Plant Biotechnol J* 19, 1086-1088 (2021).
- 21 Ren, C. *et al.* Optimizing the CRISPR/Cas9 system for genome editing in grape by using grape promoters. *Hortic Res* **8**, 52 (2021).
- Jinek, M. *et al.* A programmable dual RNA-guided DNA endonuclease in adaptive bacterial immunity. *Science* **337**, 816-21 (2012).
- Zetsche, B. *et al.* Cpf1 is a single RNA-guided endonuclease of a class 2 CRISPR-Cas system. *Cell* **163**, 759-771 (2015).
- Ming, M. *et al.* CRISPR-Cas12b enables efficient plant genome engineering. *Nat Plants* **6**, 202-208 (2020).
- Tang, X. *et al.* A CRISPR-Cpf1 system for efficient genome editing and transcriptional repression in plants. *Nat Plants* **3**, 17018 (2017).
- Zhong, Z. *et al.* Plant Genome Editing Using FnCpf1 and LbCpf1 Nucleases at Redefined and Altered PAM Sites. *Mol Plant* 11, 999-1002 (2018).
- Wang, Q. *et al.* The application of a heat-inducible CRISPR/Cas12b (C2c1) genome editing system in tetraploid cotton (G. hirsutum) plants. *Plant Biotechnol J* **18**, 2436-2443 (2020).
- Zhang, Y. et al. Expanding the scope of plant genome engineering with Cas12a orthologs and highly multiplexable editing systems. *Nat Commun* 12, 1944 (2021).
- 29 Konermann, S. *et al.* Genome-scale transcriptional activation by an engineered CRISPR-Cas9 complex. *Nature* **517**, 583-588 (2015).
- Lowder, L. G. *et al.* A CRISPR/Cas9 Toolbox for Multiplexed Plant Genome Editing and Transcriptional Regulation. *Plant Physiol* **169**, 971-985 (2015).
- Chavez, A. *et al.* Comparison of Cas9 activators in multiple species. *Nat Methods* **13**, 563-567 (2016).
- Li, Z. *et al.* A potent Cas9-derived gene activator for plant and mammalian cells. *Nat Plants* **3**, 930-936 (2017).
- Liao, H. K. *et al.* In Vivo Target Gene Activation via CRISPR/Cas9-Mediated Trans-epigenetic Modulation. *Cell* **171**, 1495-1507 e1415 (2017).
- Lowder, L. G. *et al.* Robust Transcriptional Activation in Plants Using Multiplexed CRISPR-Act2.0 and mTALE-Act Systems. *Mol Plant* 11, 245-256 (2018).
- 35 Pan, C. et al. CRISPR-Act3.0 for highly efficient multiplexed gene activation in plants. Nat

- Plants 7, 942-953 (2021).
- Wu, J. *et al.* The genome of the pear (Pyrus bretschneideri Rehd.). *Genome Res* **23**, 396-408 (2013).
- Charrier, A. *et al.* Efficient Targeted Mutagenesis in Apple and First Time Edition of Pear Using the CRISPR-Cas9 System. *Front Plant Sci* **10**, 40 (2019).
- Cheng, J. *et al.* A single nucleotide mutation in GID1c disrupts its interaction with DELLA1 and causes a GA-insensitive dwarf phenotype in peach. *Plant Biotechnol J* **17**, 1723-1735 (2019).
- Yao, G. *et al.* Map-based cloning of the pear gene MYB114 identifies an interaction with other transcription factors to coordinately regulate fruit anthocyanin biosynthesis. *Plant J* **92**, 437-451 (2017).
- 40 Lu, S. *et al.* The Citrus Transcription Factor CsMADS6 Modulates Carotenoid Metabolism by Directly Regulating Carotenogenic Genes. *Plant Physiol* **176**, 2657-2676 (2018).
- 41 An, J. P. *et al.* Apple bZIP transcription factor MdbZIP44 regulates abscisic acid-promoted anthocyanin accumulation. *Plant Cell Environ* **41**, 2678-2692 (2018).
- Bai, S. *et al.* BBX16, a B-box protein, positively regulates light-induced anthocyanin accumulation by activating MYB10 in red pear. *Plant Biotechnol J* 17, 1985-1997 (2019).
- Bai, S. *et al.* Two B-box proteins, PpBBX18 and PpBBX21, antagonistically regulate anthocyanin biosynthesis via competitive association with Pyrus pyrifolia ELONGATED HYPOCOTYL 5 in the peel of pear fruit. *Plant J* 100, 1208-1223 (2019).
- 44 Xue, C. *et al.* PbrMYB169 positively regulates lignification of stone cells in pear fruit. *J Exp Bot* **70**, 1801-1814 (2019).
- Wang, R. *et al.* A systems genetics approach reveals PbrNSC as a regulator of lignin and cellulose biosynthesis in stone cells of pear fruit. *Genome Biol* **22**, 313 (2021).
- Tao, S., Khanizadeh, S., Zhang, H. & Zhang, S. Anatomy, ultrastructure and lignin distribution of stone cells in two Pyrus species. *Plant Science* **176**, 413-419 (2009).
- 47 Papikian, A., Liu, W., Gallego-Bartolome, J. & Jacobsen, S. E. Site-specific manipulation of Arabidopsis loci using CRISPR-Cas9 SunTag systems. *Nat Commun* **10**, 729 (2019).
- Liu, H. *et al.* The involvement of PybZIPa in light-induced anthocyanin accumulation via the activation of PyUFGT through binding to tandem G-boxes in its promoter. *Hortic Res* **6**, 134 (2019).
- Bae, S., Park, J. & Kim, J. S. Cas-OFFinder: a fast and versatile algorithm that searches for potential off-target sites of Cas9 RNA-guided endonucleases. *Bioinformatics* **30**, 1473-1475 (2014).
- Nishitani, C. *et al.* Efficient Genome Editing in Apple Using a CRISPR/Cas9 system. *Sci Rep* **6**, 31481 (2016).
- Zhou, J., Wang, G. & Liu, Z. Efficient genome editing of wild strawberry genes, vector development and validation. *Plant Biotechnol J* **16**, 1868-1877 (2018).
- Xing, H.-L. *et al.* A CRISPR/Cas9 toolkit for multiplex genome editing in plants. *BMC Plant Biol* **14**, 327 (2014).
- Ren, Q. *et al.* Improved plant cytosine base editors with high editing activity, purity, and specificity. *Plant Biotechnol J* **19**, 2052-2068 (2021).
- Lee, K. *et al.* Activities and specificities of CRISPR/Cas9 and Cas12a nucleases for targeted mutagenesis in maize. *Plant Biotechnol J* **17**, 362-372 (2019).

- Li, J. et al. Efficient multiplex genome editing by CRISPR/Cas9 in common wheat. *Plant Biotechnol J* **19**, 427-429 (2021).
- Randall, L. B. *et al.* Genome- and transcriptome-wide off-target analyses of an improved cytosine base editor. *Plant Physiol* **187**, 73-87 (2021).
- Jia, H. & Wang, N. Targeted genome editing of sweet orange using Cas9/sgRNA. *PLoS One* **9**, e93806 (2014).
- Nakajima, I. *et al.* CRISPR/Cas9-mediated targeted mutagenesis in grape. *PLoS One* **12**, e0177966 (2017).
- Wang, Z. et al. Optimized paired-sgRNA/Cas9 cloning and expression cassette triggers high-efficiency multiplex genome editing in kiwifruit. Plant Biotechnol J 16, 1424-1433 (2018).
- Kaur, N. et al. CRISPR/Cas9-mediated efficient editing in phytoene desaturase (PDS) demonstrates precise manipulation in banana cv. Rasthali genome. Funct Integr Genomics 18, 89-99 (2018).
- Naim, F. *et al.* Gene editing the phytoene desaturase alleles of Cavendish banana using CRISPR/Cas9. *Transgenic Res* **27**, 451-460 (2018).
- King, S. et al. CRISPR/Cas9-introduced single and multiple mutagenesis in strawberry. J Genet Genomics 45, 685-687 (2018).
- Wilson, F. M., Harrison, K., Armitage, A. D., Simkin, A. J. & Harrison, R. J. CRISPR/Cas9-mediated mutagenesis of phytoene desaturase in diploid and octoploid strawberry. *Plant Methods* **15**, 45 (2019).
- Wang, X. *et al.* CRISPR/Cas9-mediated efficient targeted mutagenesis in grape in the first generation. *Plant Biotechnol J* **16**, 844-855 (2018).
- Martin-Pizarro, C., Trivino, J. C. & Pose, D. Functional analysis of the TM6 MADS-box gene in the octoploid strawberry by CRISPR/Cas9-directed mutagenesis. *J Exp Bot* **70**, 885-895 (2019).
- Peng, A. *et al.* Engineering canker-resistant plants through CRISPR/Cas9-targeted editing of the susceptibility gene CsLOB1 promoter in citrus. *Plant Biotechnol J* **15**, 1509-1519 (2017).
- Wang, M., Mao, Y., Lu, Y., Tao, X. & Zhu, J. K. Multiplex Gene Editing in Rice Using the CRISPR-Cpfl System. *Mol Plant* 10, 1011-1013 (2017).
- 68 Li, B. *et al.* Robust CRISPR/Cpf1 (Cas12a)-mediated genome editing in allotetraploid cotton (Gossypium hirsutum). *Plant Biotechnol J* 17, 1862-1864 (2019).
- Li, B. et al. The application of temperature sensitivity CRISPR/LbCpf1 (LbCas12a) mediated genome editing in allotetraploid cotton (G. hirsutum) and creation of nontransgenic, gossypol-free cotton. *Plant Biotechnol J* 19, 221-223 (2021).
- Jia, H., Orbovic, V. & Wang, N. CRISPR-LbCas12a-mediated modification of citrus. *Plant Biotechnol J* 17, 1928-1937 (2019).
- Malzahn, A. A. *et al.* Application of CRISPR-Cas12a temperature sensitivity for improved genome editing in rice, maize, and Arabidopsis. *BMC Biol* **17**, 9 (2019).
- Teng, F. *et al.* Repurposing CRISPR-Cas12b for mammalian genome engineering. *Cell Discov* **4**, 63 (2018).
- Xu, J., Hua, K. & Lang, Z. Genome editing for horticultural crop improvement. *Hortic Res* **6**, 113 (2019).
- 74 Meng, X. et al. Construction of a Genome-Wide Mutant Library in Rice Using CRISPR/Cas9.

- Mol Plant 10, 1238-1241 (2017).
- Lu, Y. *et al.* Genome-wide Targeted Mutagenesis in Rice Using the CRISPR/Cas9 System. *Mol Plant* **10**, 1242-1245 (2017).
- Jacobs, T. B., Zhang, N., Patel, D. & Martin, G. B. Generation of a Collection of Mutant Tomato Lines Using Pooled CRISPR Libraries. *Plant Physiol* **174**, 2023-2037 (2017).
- Liu, H. J. *et al.* High-Throughput CRISPR/Cas9 Mutagenesis Streamlines Trait Gene Identification in Maize. *Plant Cell* **32**, 1397-1413 (2020).
- Bai, M. *et al.* Generation of a multiplex mutagenesis population via pooled CRISPR-Cas9 in soya bean. *Plant Biotechnol J* **18**, 721-731 (2020).
- An, J. P. *et al.* The bZIP transcription factor MdHY5 regulates anthocyanin accumulation and nitrate assimilation in apple. *Hortic Res* **4**, 17023 (2017).
- An, J. P. *et al.* BTB protein MdBT2 inhibits anthocyanin and proanthocyanidin biosynthesis by triggering MdMYB9 degradation in apple. *Tree Physiol* **38**, 1578-1587 (2018).
- You, Q. *et al.* CRISPRMatch: An Automatic Calculation and Visualization Tool for High-throughput CRISPR Genome-editing Data Analysis. *Int J Biol Sci* 14, 858-862 (2018).
- Yamagishi, Y. *et al.* In vitro induction of secondary xylem-like tracheary elements in calli of hybrid poplar (Populus sieboldii x P. grandidentata). *Planta* **237**, 1179-1185 (2013).



Supplementary data

Figure S1. DNA sequence alignment of *PyPDS***.** Ref, reference. DS, 'Dangshansuli' pear fruits. Callus, dedifferentiated 'Clapp's Favorite' pear calli. Qiuzili, pear plants for tissue culture.

Figure S2. DNA sequence alignment of *PyGID1.* Ref, reference. DS, 'Dangshansuli' pear fruits. Callus, dedifferentiated 'Clapp's Favorite' pear calli. Qiuzili, pear plants for tissue culture.

Figure S3. DNA sequence alignment of *PyTFL1.1/1.2.* REF, reference. DS, 'Dangshansuli' pear fruits. Callus, dedifferentiated 'Clapp's Favorite' pear calli. Qiuzili, pear plants for tissue culture.

Figure S4. Guide RNA design and construction of CRISPR/Cas9 vectors for genome editing. A, Schematics of the sgRNA positions and sequences. *PyPDS*, *PyGID1* and *PyTFL1.1/1.2* are target genes for genome editing. The 20 nt protospacers with an NGG PAM are designed for Cas9. B, Vectors of different CRISPR/Cas9 systems for genome editing.

Figure S5. PCR identification of the regenerated calli (pLR01-16) using vector-specific primers. M, DNA marker. Plasmid, positive control. WT, wide type. H₂O, negative control.

Figure S6. PCR identification of the regenerated calli (pLR55-64) using vector-specific primers. A, M, DNA marker. Plasmid, positive control. WT, wide type. H₂O, negative control. B, Reconstructed vectors with hygromycin gene replaced with kanamycin gene.

Figure S7. Mutation frequencies at *PyPDS***-gRNA05 site by PCR-RFLP and Sanger sequencing analysis.** A, PCR-RFLP analysis of CRISPR/Cas9-induced mutation at the *PyPDS*-gRNA05 site. The PflmI enzyme site used for PCR-RFLP analysis is highlighted in green. Mutation frequencies were calculated by Image J. B, Sanger sequencing analysis CRISPR/Cas9-induced mutation at the *PyPDS*-gRNA05

site. Dash indicates 1 bp deletion. Green DNA bases indicate insertion. The PAM sequence is highlighted in red, and the target sequence is highlighted in blue. WT, wild-type sequence.

Figure S8. The deletion and insertion frequency of CRISPR/Cas9 system with 35S and AtU3 promoters at target sites of *PyPDS* and *PyGID1*. A, *PyPDS*. B, *PyGID1*.

Figure S9. DNA sequence alignment of *PyMYB10* and *PyMYB114*. REF, reference. CALLUS, dedifferentiated 'Clapp's Favorite' pear calli.

Figure S10. Guide RNA design and construction of CRISPR/Cas12a and Cas12b vectors for genome editing. A, Schematics of the crRNA and sgRNA positions and sequences for CRISPR/Cas12a and Cas12b systems. For Cas12a, 23 nt protospacers with a TTTV PAM are designed. For Cas12 b, 20 nt protospacers with a VTTV PAM are designed. B, Vector constructions of CRISPR/Cas12a and Cas12b systems.

Figure S11. PCR identification of the regenerated calli (pLR67-83) using vector-specific primers. M, DNA marker. Plasmid, positive control. WT, wide type. H₂O, negative control.

Figure S12. DNA sequence alignment of *PyMYB169* **and** *PyNSC.* REF, reference. DS, 'Dangshansuli' pear fruits. CALLUS, dedifferentiated 'Clapp's Favorite' pear calli.

Figure S13. Guide RNA design for anthocyanin and lignin biosynthetic genes knockout by CRISPR/Cas9. A, Schematics of the sgRNA positions and sequences of *PyMYB10*, *PyMYB114*, *PyMYB169* and *PyNSC* for genome editing. For Cas9, 20 nt protospacers with a NGG PAM are designed. B, Vector construction of CRISPR/Cas9 system for anthocyanin and lignin engineering.

Figure S14. PCR identification of the regenerated calli (pLR89-94) using vector-specific primers. M, DNA marker. Plasmid, positive control. WT, wide type. H₂O, negative control.

Figure S15. Sanger sequencing results (pLR89-91). The number represent mutated clones / sequenced clones. Dash indicates 1 bp deletion. Green DNA bases indicate insertion. The PAM sequence is highlighted in red, and the target sequence is highlighted in blue. WT, wild-type sequence.

Figure S16. Sanger sequencing results (pLR92, 94). The number represent mutated clones / sequenced clones. Dash indicates 1 bp deletion. Green DNA bases indicate insertion. The PAM sequence is highlighted in red, and the target sequence is highlighted in blue. WT, wild-type sequence.

Figure S17. Guide RNA design for CRISPRa-based transcriptional activation. A, Schematics of the sgRNA positions and sequences of *PybZIPa*, *PyMYB114*, *PyMYB10*, *PybHLH3*, *PyDFR*, *PyANS* and *PyUFGT* for transcriptional activation. 20 nt protospacers with a NGG PAM are designed for Cas9. B, Vector construction of CRISPRa system for transcriptional activation of anthocyanin pathway genes.

Figure S18. PCR identification of the regenerated calli (pLR47-54) using vector-specific primers. M, DNA marker, Plasmid, positive control. WT, wide type. H₂O, negative control.

Figure S19. Sanger sequencing analysis of putative off-target sites for CRISPR/Cas9. The number represent mutated clones / sequenced clones. Dash indicates 1 bp deletion. Green DNA bases indicate insertion. The PAM sequence is highlighted in red, and the target sequence is highlighted in blue. WT, wild-type sequence.

Supplementary Table S1. All primers used in this study.

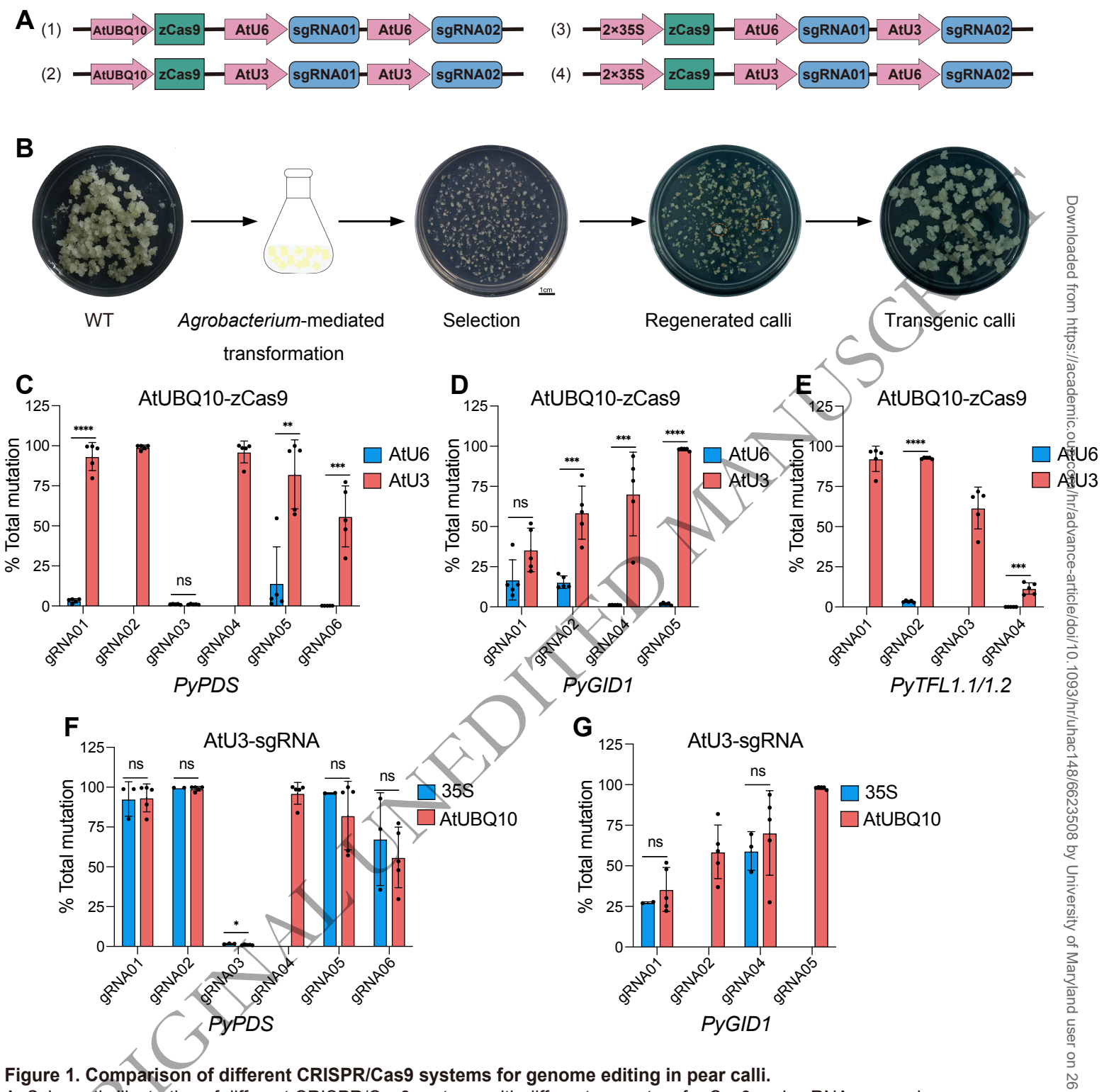


Figure 1. Comparison of different CRISPR/Cas9 systems for genome editing in pear calli.

A, Schematic illustration of different CRISPR/Cas9 systems with different promoters for Cas9 and sgRNA expression.

AtUBQ10, Arabidopsis ubiquitin promoter; 35S, CAMV 35S promoter; AtU3, Arabidopsis U3 promoter; AtU6, Arabidopsis U6 promoter; zCas9, maize codon optimized SpCas9.

- B, Stable transformation of pear calli. WT, wide-type pear calli. A mass of regenerated calli highlighted by orange dotted circle is considered as an independent stable line.
- C-E, Comparison of mutation frequencies of AtU3- and AtU6-based sgRNAs expression for CRISPR/Cas9 systems in pear calli. zCas9 is driven by AtUBQ10 promoter. A total of six, four and four unique sgRNAs were designed for *PyPDS* (C), *PyGID1* (D) and *PyTFL1.1/1.2* (E), respectively.
- F-G, Comparison of mutation frequencies of AtUBQ10- and 35S-based Cas9 expression for CRISPR/Cas9 systems in pear calli. The sgRNAs are driven by AtU3 promoter. A total of six and four unique sgRNAs were designed for PyPDS (F) and PyGID1 (G), respectively. All data are derived from high-throughput amplicon deep sequencing and presented as the mean \pm SDs (n = 3 to 5 independent lines). ns P > 0.05, *P < 0.05, *P < 0.01, ***P < 0.001, ***P < 0.0001, ****P < 0.0001, ***

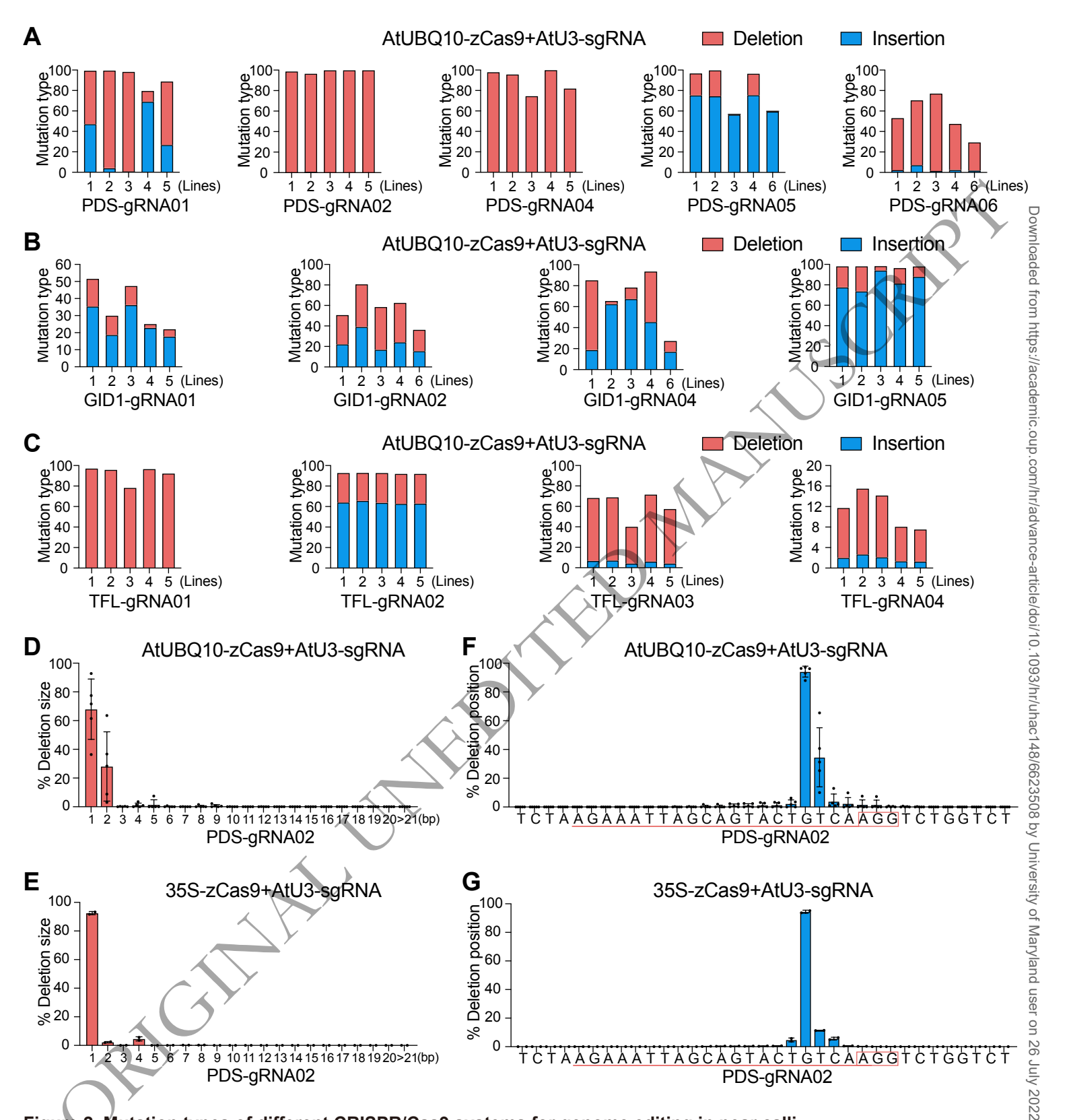


Figure 2. Mutation types of different CRISPR/Cas9 systems for genome editing in pear calli.

A-C, The deletion and insertion frequencies of CRISPR/Cas9 system with AtUBQ10 and AtU3 promoters. A total of five, four and four target sites were analyzed for *PyPDS* (A), *PyGID1* (B) and *PyTFL1.1/1.2* (C), respectively.

D-E, Comparison of deletion sizes of AtUBQ10- and 35S-based zCas9 at the *PyPDS*-gRNA02 site. The sgRNA is driven by AtU3 promoter.

F-G, Comparison of deletion position of AtUBQ10- and 35S-based zCas9 at the *PyPDS*-gRNA02 site. The sgRNA is driven by AtU3 promoter. PAM and protospacer sequences are circled and underlined, respectively.

All data are derived from high-throughput amplicon deep sequencing and presented as the mean \pm SDs (n = 3 to 5 independent lines).

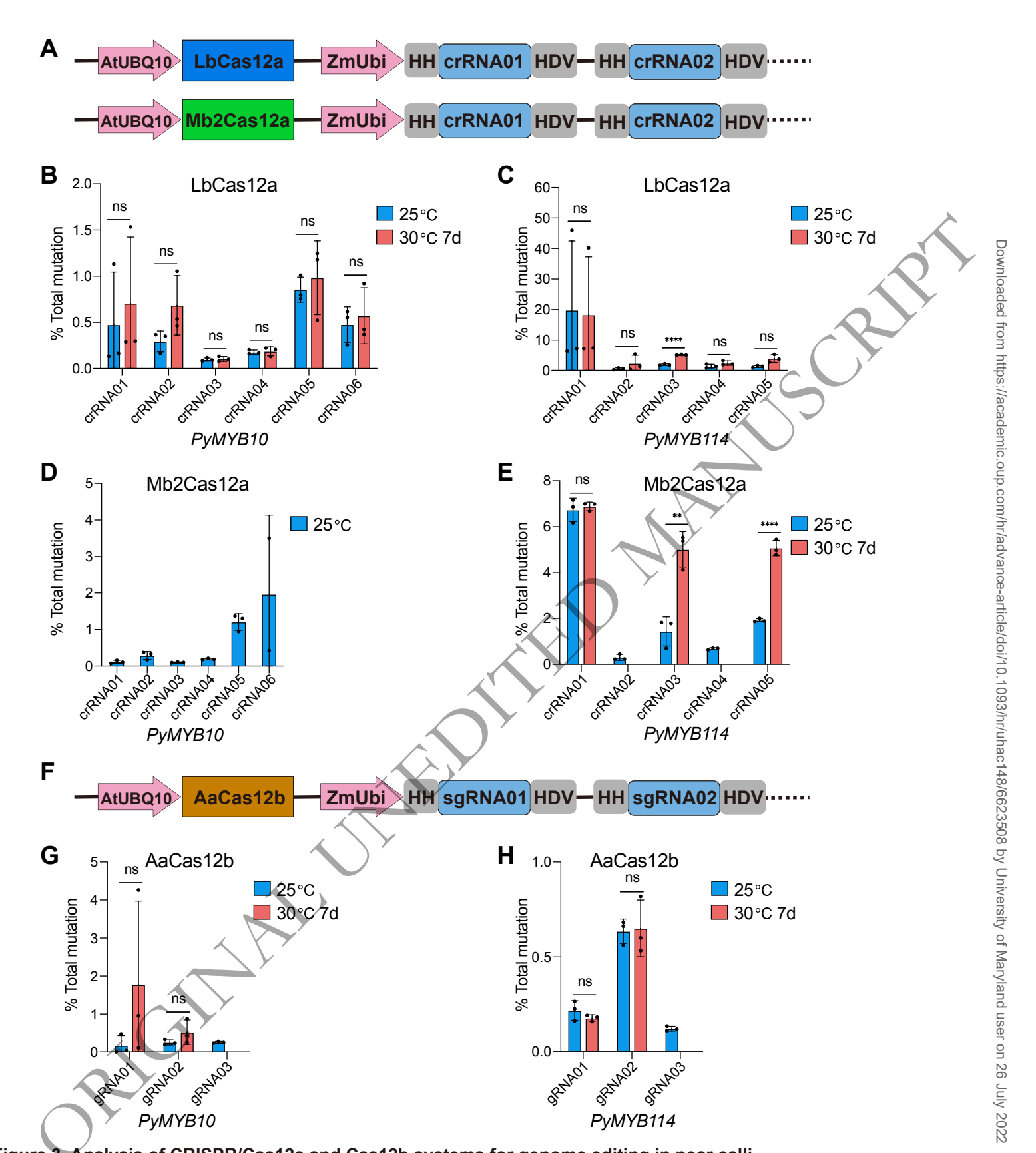


Figure 3. Analysis of CRISPR/Cas12a and Cas12b systems for genome editing in pear calli.

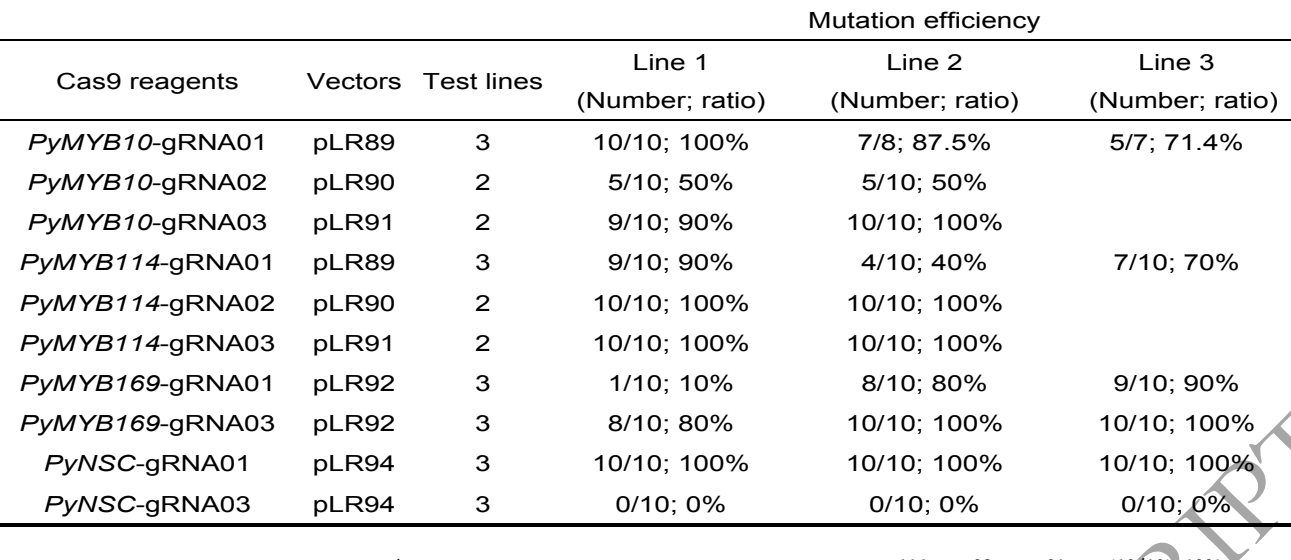
A, Schematic illustration of the dual Pol II promoter system for expression of Cas12a and crRNAs. AtUBQ10, *Arabidopsis* ubiquitin promoter; ZmUbi, maize ubiquitin promoter; HH, hammerhead ribozyme; HDV, hepatitis delta virus ribozyme.

B-E, Analysis of mutation frequencies of LbCas12a (B, C) and Mb2Cas12a (D, E) at 25 °C and 30 °C in stable pear calli. Six and five different crRNAs were designed for *PyMYB10* (B, D) and *PyMYB114* (C, E), respectively.

F, Schematic illustration of the dual Pol II promoter system for expression of Cas12b and sgRNAs.

G-H, Analysis of mutation frequencies of AaCas12b at 25°C and 30°C in stable pear calli. Three different sgRNAs were designed for *PyMYB10* (G) and *PyMYB114* (H), respectively.

All data are derived from high-throughput amplicon deep sequencing and presented as the mean \pm SDs (n = 3 independent lines). ns P > 0.05, *P < 0.05, *P < 0.01, ***P < 0.001, ***P < 0.001, ***P < 0.0001, ***P < 0.



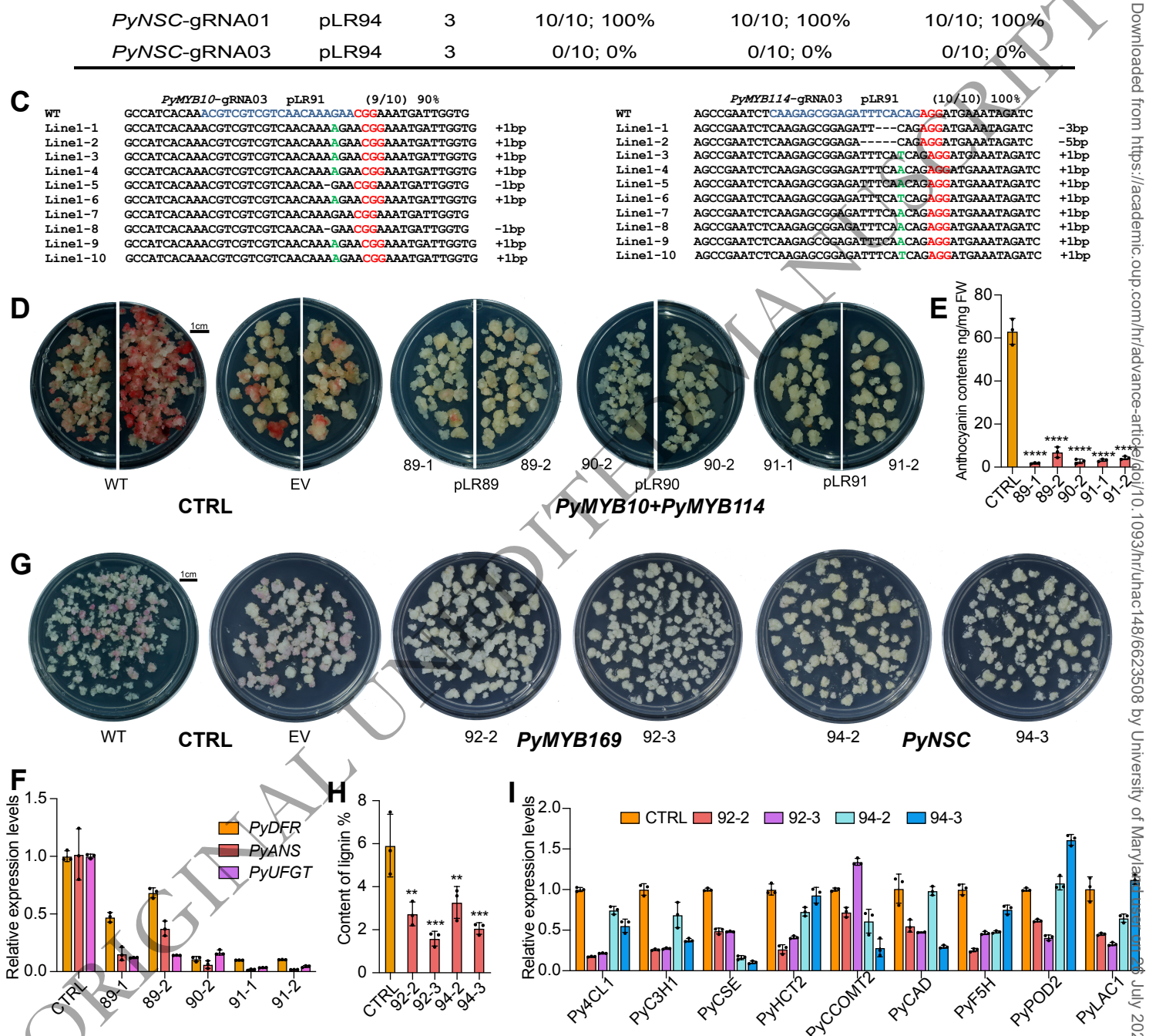


Figure 4. Multiplexed anthocyanin and lignin biosynthetic genes knockout by CRISPR/Cas9 system in pear calli.

A, Schematic illustration of CRISPR/Cas9 system for multiplexed gene or site knockout in pear calli.

- B, Summary of mutation results of CRISPR/Cas9 system at different sites in stable pear calli. The mutation efficiencies were generated using Sanger sequencing. The number represents mutated clones / sequenced clones.
- C, The mutation type and frequency of each mutation at the *PyMYB10*-gRNA03 and *PyMYB114*-gRNA03 sites. The PAM sequence is highlighted in red, and the target sequence is highlighted in blue. WT, wild-type sequence. Dash indicates 1 bp deletion. Green DNA bases indicate insertion.
- D, Phenotypes of *PyMYB10* and *PyMYB114* knockout calli with continuous light treatment for 7 days. Treatment medium: MS solid medium without nitrogen but containing 200 µM/L of Methyl jasmonate (MeJA).
- E, Anthocyanin contents of CRISPR/Cas9-mediated and CTRL pear calli.
- F, Relative transcript level of anthocyanin biosynthetic genes in CRISPR/Cas9-mediated and CTRL pear calli.
- G, Phenotypes of PyMYB169 or PyNSC knockout calli with continuous dark treatment for 20 days.
- H, Lignin contents in CRISPR/Cas9-mediated and CTRL pear calli.
- I, Relative transcript level of lignin biosynthetic genes in CRISPR/Cas9-mediated and CTRL calli.

The WT calli and calli harboring T-DNA vector without sgRNA (EV) were used as controls (CTRL). PyGAPDH was used as the endogenous control gene. All data are presented as the mean \pm SDs (n=3 independent experiments). ns P > 0.05, *P < 0.05, *P < 0.01, ***P < 0.001, **P < 0.001, ***P < 0.001,

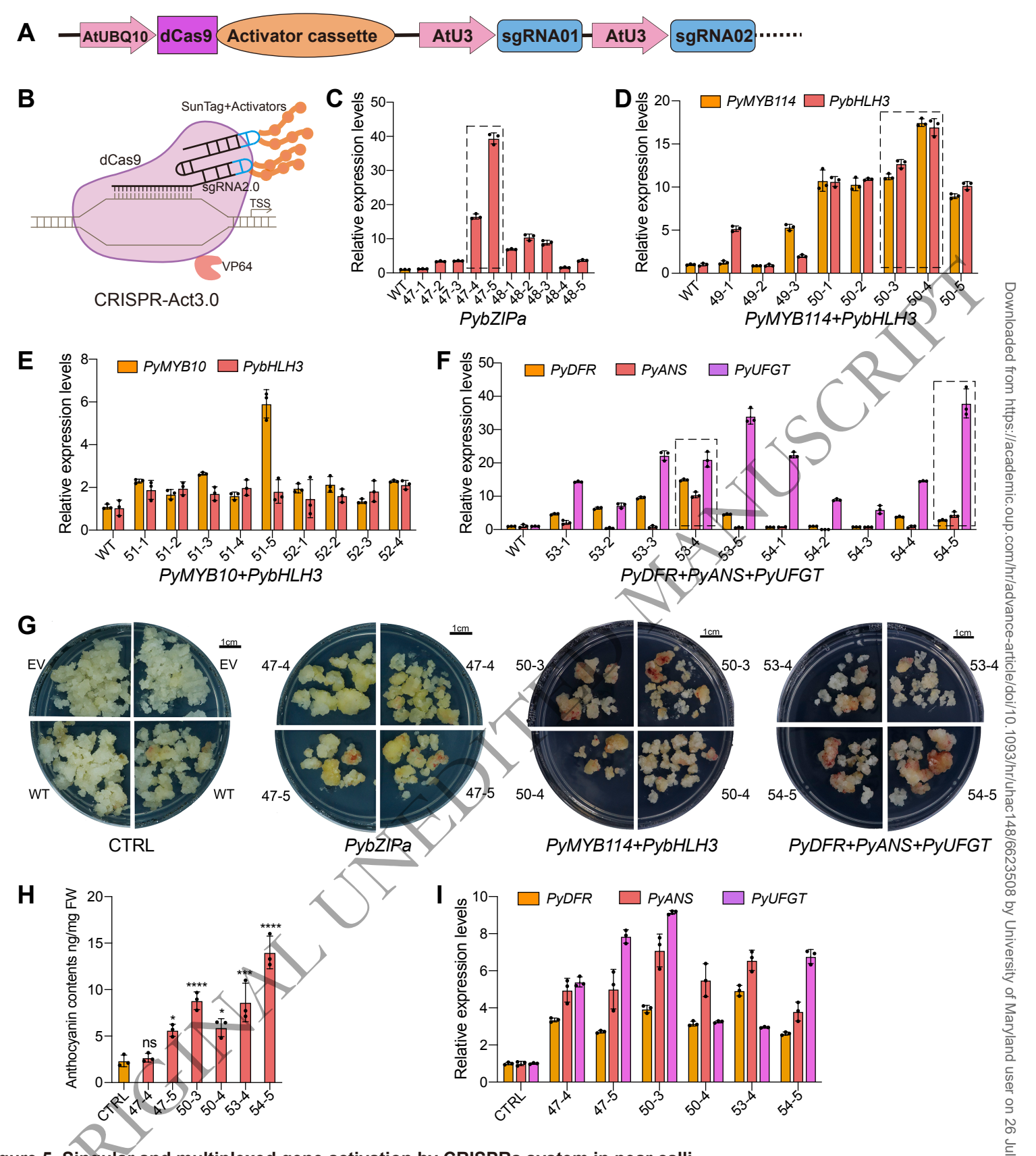


Figure 5. Singular and multiplexed gene activation by CRISPRa system in pear calli.

A, Schematic illustration of CRISPRa system used in pear calli for singular and multiplexed gene activation. AtUBQ10, Arabidopsis ubiquitin promoter; AtU3, Arabidopsis U3 promoter; dCas9, deactivated zCas9.

- B, A schematic diagram of activator cassette in CRISPR-Act3.0.The dCas9 is fused with a VP64, the sgRNA2.0 scaffold contains two MS2 RNA aptamers (in blue), SunTag+Activators contain 10×GCN4 SunTag, a scFV,a sfGFP, and 2×TAD activator.
- C-F, CRISPRa-mediated activation of one (C), two (D, E) and three (F) anthocyanin biosynthetic genes in calli. Three to five independent transgenic lines were used in each experiment. The stable lines highlighted in the black dotted box were chosen for phenotype analysis.
- G, Phenotypes of CRISPRa-mediated and CTRL pear calli with continuous light treatment for 12 days. Treatment medium: MS solid medium containing 50 μM/L of MeJA.
- H, Anthocyanin contents of CRISPRa-mediated and CTRL pear calli.
- I, Relative transcript level of anthocyanin biosynthetic genes in CRISPRa-mediated and CTRL calli.
- The WT calli and calli harboring T-DNA vector without sgRNA (EV) were used as control (CTRL). PyGAPDH was used as the endogenous control gene. All data are presented as the mean \pm SDs (n=3 independent experiments). ns P > 0.05, *P < 0.05, *P < 0.01, ***P < 0.001, ***P < 0.0001, two-tailed Student's t-tests.

Table 1. Off-target analysis of CRISPR/Cas9 system in pear calli.

A total of ten potential off-target sites were analyzed. The PAM sequence is highlighted in red, and the mismatch base is highlighted in green lowercase. The off-target ratios were generated from Sanger sequencing results. The number represents mutated clones / sequenced clones.

Target genes	sgRNA sequences	Putative off-target sequences	Mismatch number	Test vectors; lines	Off-target ratio (Number; ratio)
PyPDS-gRNA02	AGAAATTAGCAGTACTGTCAAGG	AGAAATTAaCAGcACTcTCA <mark>TGG</mark>	3	pLR04; Line1	0/5; 0%
PyGID1-gRNA05	CTCGCTGGCGATAGCTCGGGTGG	CTaGCTGGCGATAGCTCtGGCGG	2	pLR10; Line1	2/5; 40%
PyTFL1.1-gRNA03	GAGATGCCGAAGCCCAATATTGG	GAGATGCCaAgGCCCAAcATTGG	3	pLR14; Line1	0/5; 0%
PyMYB10-gRNA03	ACGTCGTCGTCAACAAAGAACGG	ACGTCGTCGTCGACAAAcAATGG	2	pLR91; Line1	0/5; 0%
		ACGTtGTCaTCgACAAAGAATGG	3	pLR91; Line1	0/5; 0%
		tCtTCaTCGTCAACAAAGAATGG	3	pLR91; Line1	0/5; 0%
		ACGTCGTCGTtgACAAAcAATGG	3	pLR91; Line1	0/5; 0%
<i>PyMYB114</i> -gRNA03	CAAGAGCGGAGATTTCACAGAGG	aAAGAtCGGAGATTTCACAG <mark>TGG</mark>	2	pLR91; Line1	3/5; 60%
		CAAaAGCGGACATTTtACAGAGG	3	pLR91; Line1	0/5; 0%
		CAAGAGaGGAGACTTtACAGAGG	3	pLR91; Line1	0/5; 0%

Downloaded from https://academic.oup.com/hr/advance-article/doi/10.1093/hr/uhac148/6623508 by University of Maryland user on 26 July 2022